Egypt. J. Chem. **Vol. 67** No. 10 pp. 77- 86 (2024)

Egyptian Journal of Chemistry

http://ejchem.journals.ekb.eg/

A-10 kGy of γ-irradiation enhanced the techno-functional properties of psyllium seed's fiber via maximizing the surface and altering the structure

Mohamed Mowafi[a,b], Ibrahim Khalifa[a*], Ashraf M. Mounir[b], Mahmoud Hassan[a], Hammam Bahlol[a]

[a]Food Technology Department, Faculty of Agriculture,13736, Moshtohor, Benha University, Egypt.
[b]Food Irradiation Research Dept., National Centre for Radiation Research and Technology (NCRRT), Atomic Energy Authority, Cairo, Egypt.

Abstract

The major source of raw materials for the experiment was Psyllium fiber (PF), an insoluble diet fiber derived from Psyllium seeds. The key composition, particle size and specific surface area, microstructure by SEM, FTIR, and X-ray diffraction of PF were all examined concerning the impact of irradiation doses of 0, 5, 10, and 20 kGy. Results implied that when the dose of γ-irradiation was 20 kGy equated to the untreated one, the concentrations of cellulose, hemicellulose, and lignin in PF fell by 13.74, 23.41, and 16.6%, orderly, and the volume particle size of PF declined by 130.44 μm. The specific surface area expanded by 83.28 m2/kg while the crystallinity slightly declined. Pores and erratic particles could be seen on the PF's microstructure surface after exposure to γ-irradiation. According to the IR-spectrum data, the hemicellulose and lignin in PF were eliminated by γ-irradiation. These results indicate that the structural properties of PF may be significantly affected by γ-irradiation. When the radiation dosage was 10 kGy, PF had the greatest oil-holding, H_2O-holding, and swelling capabilities (8.35 g/g, 21.0 g/g, and 9.35 mL/g, respectively), and it also had the strongest adsorption capacities for sodium nitrate, cholesterol, and glucose. These results imply that γ-irradiation improves the PF's functional properties. This study's use of γ-irradiation technology as a pre-treatment provided a theoretical framework for the use of PF in food processing.

Keywods: Psyllium fiber; gamma radiation; techno-functional properties; mechanism

1. Introduction

According to Alabaster et al. [1], psyllium is a plant with a high proportion of H_2O-soluble fiber that has a multitude of health benefits, pharmacological qualities, and good nutritional impacts. The popular term found in the seed of an annual plant belonging to the Plantago genus, which has over 200 distinct species, is psyllium. Freshly, its usage in Europe has expanded, and it is now widely consumed in the USA as well [2]. By mechanically milling, or grinding the seed's outer covering, mucilage is made from the coat of psyllium (*P. ovata*) seeds. According to Verma et al. [3], the term "mucilage" refers to a class of transparent, colorless gelling agents originating from plants. Due to its reputation as an excellent source of both soluble and insoluble fiber and its status as a naturally occurring, medicinally potent gel-forming polysaccharide, psyllium mucilage has a long history as a nutritional supplement [4]. Due to its large water-holding capacity, which is around 80 times its weight, this mucilage gels and is well recognized for its laxative effects [5]. Numerous studies on psyllium's possible health advantages and uses in the food and pharmaceutical sectors have been conducted [6-8]. Because of its potent hydrophilic and gelling qualities, stabilizing, suspending, and emulsifying abilities, psyllium seed husk, a well-known source for the synthesis of psyllium hydrocolloid, also serves practical use in food.

Fibers have large molecular weights and are thus anticipated to be effective viscosity enhancers [9]. Standard foods enriched with PF, such as biscuits and yogurt, have been described in supplements and the development of food products as well as in the production of low-calorie and low-fat food as well as a substitute for gluten [5]. PF is also widely used in a variety of other industries, including cosmetics (for the

*Corresponding author e-mail: ibrahiem.khalifa@fagr.bu.edu.eg.; (Ibrahim Khalifa).
Receive Date: 01 January 2024, Revise Date: 12 March 2024, Accept Date: 27 March 2024
DOI: 10.21608/ejchem.2024.251484.9003

provision of hair and skin care products) and supplements for weight control [10,11]. However, when the unmodified insoluble dietary fiber is directly incorporated into baked food, meat products, beverage products, jams, and other fields, it will affect their sensory quality and physical [2,12]. To enhance the processing qualities and application quality of the insoluble dietary fiber in psyllium, a novel method should be used.

In this context, cold sterilization using γ-irradiation has several advantages, including easy control, no chemical needs, quick processing times, huge processing capacities, and no environmental contamination with several potential applications in the industrial production [13]. The WTO declared that there is no risk to food when the irradiation dosage is larger than 10 kGy [14]. Irradiation therapy in the food industry is now mostly used to sterilize food, modify proteins, remove enzymes, increase fiber breakdown, and in other applications. It has been discovered that γ-irradiation changes the structure of the polymer by producing several intermediates that go through a variety of quick reaction routes and add new bonds to the chain [15]. Studies by Fei, et al. [16] and Li, et al. [17] discovered a rise in radiation exposure, the depolymerization of hemicellulose, cellulose, lignin, and the correlation between a change in dietary fiber and a cracking structure. Additionally, they discovered that as the free group grew, dietary fiber in its crystalline and amorphous forms was eliminated and that a greater proportion of crystalline form was broken down into an amorphous form. This decreased thermal stability, polymerization level, and crystallinity. The dietary fiber was also degraded by combining γ-irradiation with micropulverization [18]. It was then suggested that γ-irradiation is a potentially useful approach for modifying fiber structure and enhancing fiber performance. Meanwhile, few publications on how γ-irradiation affects the physicochemical features and usefulness of dietary fiber derived from PF. To investigate the impacts of γ-irradiation doses (0, 5, 10, and 20 kGy) on the physicochemical and functional features of PF, raw PF was employed as a raw material herein. A theoretical foundation for the widespread industrial use of PF in the future is provided by this work as well.

2. Experimental

Material and reagents

Psyllium fiber (PF) was obtained from a market for herbal located in Toukh, Qaluobia, Egypt. KBr (Beijing Chemical Reagent Factory, Beijing, China), Naphthalene hydrochloride (Tianjin Dongli Tianda Chemical Reagent Factory, Tianjin, China), P-aminobenzene sulfonic acid (Nanjing Chemical Reagent Company, Nanjing, China), Dinitrosalicylate (DNS), nitrite, and glucose (Sigma Chemical Company, St. Louis, MO; USA).

Preparation of irradiated-PF

The Egyptian Atomic Authority cobalt source facility served as the site for the radiation test (activity: 200 kCi; temperature: 20 1 °C; average dose rate: 10 Gy/h; inhomogeneity: 5%). The high-speed mill was used to smash the dried PF samples before they were sieved over a 60-mesh screen. The materials were placed in plastic Ziplock bags before the irradiation tests were conducted. The radiation dosages were, correspondingly, 0, 5, 10, and 20 kGy. A silver dichromate chemical dosimeter was used to monitor the samples' exposure to radiation, and a UV-visible spectrophotometer was used to assess the dosage that was absorbed. Following irradiation, samples were kept at room temperature in sealed polyethylene bags.

Determination of PF's structural features

Determination of the key elements

The lignin was produced using an acid approach (H_2SO_4 72% v/v for 1 h), whereas cellulose and hemicellulose were produced using an alkali method (KOH 24% w/v for 2 h and KOH 10% w/v for 16 h). Hemicellulose was dried at 60 °C for 24 h after the separated cellulose and lignin had been dried at 105 °C for 2 h [19]. A commercial kit (AOAC Method 991.43) was used to evaluate the total dietary fiber (TDF), soluble dietary fiber (SDF), and insoluble dietary fiber (IDF) [18]. To eliminate the PF's protein and starch, it was continually treated with thermostable α-amylase, protease, and amyloglucosidase. The enzymatic hydrolysate was then filtered through a Celite-containing crucible, and the leftover material was twice washed with dH_2O that had been heated to 70 °C. IDF was produced by drying the crucible waste at 103 °C, the rinse solution was combined with 95% EtOH at 60 °C at a ratio of 1:4 (v/v), filtered, and then dried at 103 °C for SDF. TDF was determined by combining between IDF and SDF.

Determination of particle size and specific surface area

To assess the volume-average particle size and specific surface area of PF, a 3 g sample was dissolved in 100% EtOH and ultrasonically dispersed for 3 min using an MS2000 Masterizer particle-size analyzer (Malvern business, Malvern, UK) [20].

Microstructure's recognizing

The microstructure of irradiated and non-irradiated PF was portrayed using a scanning electron microscope (SEM) with the use of an SU8010 field emission from Hitachi in Japan [21]. Palladium was applied to PF's particles which were around 1 mg in size, on the tape of the circular aluminium sample sub for 90 s at a

current of 15 mA. The observation room was then filled with the specimen stubs. At a 10 and 200x rise and a 5 kV accelerator voltage, these PF's particles were detected.

Measuring the Fourier transform infrared spectroscopy (FTIR)

The PF and KBr (1: 250 w/w) were thoroughly combined and formed into a disk in accordance with Khalifa, et al. [22] procedures. The Scimitar 2000 FTIR spectrometer (Agilent, Santa Clara, CA, US) was then used to acquire the PF's IR-spectra with a wave number of 400-4000 cm^{-1}. There were 32 scans done on each sample.

Measuring the X-ray Diffraction (XRD)

XRD of the PF crystal structure determination was measured via an XPert Powder Multifunctional Powder X-ray Diffractometer from Dandong Tonda Technology Co., Ltd. China [23]. The scanning was done from 10 to 40° (2θ) at 1/min. The incident current was 40 mA, while the generating voltage was 40 kV.

Measuring the PF's functional features

Measuring the oil-holding capacity (OHC)

5 mL of soybean oil and 0.5 g (M0) of PF were combined. The PF were spun for 20 min at 4000 rpm in a chilled high-speed centrifuge (X1R, Thermo Fisher Scientific, MA, US) after being in a centrifuge tube for 24 h. The supernatant was removed and M1 was recorded as the weight of the residue. OHC was expressed using the next equation [24]:

$$\text{OHC (g/g)} = M_1 - M_0 / M_0 \quad (1)$$

M0 and M1 are the weights of PF (g) before and after oil absorption, separately.

Measuring the swelling (SC) and water-holding capacity (WHC)

The PF suspension was hydrated for 24 h after being diluted from 0.3 g (m0) to 15 mL (V0) with dH_2O [25]. The volume was then recorded as V1. The PF suspension was then centrifuged for 20 min at 6000 rpm. Wet fiber weight, m1, was measured after the supernatant was removed. SC and WHC were then calculated using the next formulas:

$$\text{SC (mL/g)} = V_1 - V_0 / m_0 \quad (2)$$

$$\text{WHC (g/g)} = m_1 - m_0 / m_0 \quad (3)$$

V0 is the PF dilution volume of 15 mL, V1 is the volume of the suspension after 24 h of PF hydration (mL), m0 and m1 are the PF weights (g) before and after H_2O-absorption, orderly.

Measuring the adsorption features

Nitrite

The adsorption capacity of PF to $NaNO_2$ was determined [26]. The circumstances of the small intestine and stomach were reproduced at pH = 7.0 and 2.0, orderly, using a 0.1 g PF added to a 5 mL $NaNO_2$ (20 g/mL) solution. The resulting mixture was then allowed to remain at RT for 2 h, centrifuged for 10 min at 4800 rpm, and 0.5 mL of supernatant was then put into a glass tube. Both p-aminobenzene sulfonic acid and naphthalenediamide hydrochloride were used to measure the amounts of $NaNO_2$ in the supernatant [17]. A total of 2 mL of dH_2O was poured to the tube before adding 2 mL of p-aminobenzene sulfonic acid (4 g/mL) and 1 mL of naphthalene hydrochloride (2 g/mL) to the mixture. A 30 min was given for the solution to react at 538 nm in the dark. As a result, $NaNO_2$ amount was quantified with the aid of a standard curve and followed the next equation:

$$\text{Nitrite absorption capacity (NAC, μg/g)} = (C_1 - C_2/\text{W}) \times \text{V} \quad (5)$$

W is the PF weight (g), V is the NaNO2 solution volume (mL), and C_1 and C_2 are $NaNO_2$ concentrations in the supernatant before and after adsorption, orderly (g/L).

Cholesterol

Fresh egg yolks were tinned with dH_2O (9 times) with a continues stirring until emulsified. After mixing 25 mL of the egg yolk emulsion with 0.5 g of PF, the mixture was agitated at 37 °C for 2, 5, 10, 15, 25, 40, 60, 90, and 120 min, separately. The cholesterol level in the supernatant was assessed using a UV-2700 spectrophotometer (Shimadzu Company, Japan) and the phthalaldehyde technique after centrifugation at 4000 rpm for 15 min [27,28]. The cholesterol concentration was expressed based on its standard curve following the next equation to calculate the cholesterol adsorption capacity (CAC) of PF:

$$\text{CAC (mg/g)} = C1 - C2 / \text{W} \quad (6)$$

W is PF-weight (g), C1 and C2 are the cholesterol weights (mg) before and after adsorption.

Glucose

A 0.5 g sample of PF was made along with 100 mL solutions of glucose with concentrations of 10 and 200 mmol/L. The mixture was then agitated at 37 °C for 6 h, centrifuged for 15 min at 4000 rpm, and the PF was kept in the supernatant. Dinitro salicylate chromogenic (DNS) reagent was used to measure the amount of glucose in the supernatant. A glass tube containing 0.5 mL of supernatant was then filled with dH_2O until it held 3 mL. Then, 2 mL of DNS was added to with a continuous shaken for 6 min in a water bath at 100 °C. The glucose concentration was determined at 520 nm once the solution had reached RT to create a standard curve following the next equation to calculate the glucose adsorption capacity (GAC) of PF [29]:

$$\text{GAC (mmol/g)} = (G1 - G2 / \text{W}) \times \text{V} \quad (7)$$

W is PF-weight (g), V is the supernatant volume (mL), and G1 and G2 are the glucose concentrations before and after adsorption, orderly (mmol/g).

Statistical analysis

The results were described as means ± SD. The data were explored via one-way analysis of variance (ANOVA) in SPSS 21.0 Statistics, with post hoc

Tukey's tests for multiple variations (SPSS Inc, US). When $p< 0.05$ was present, statistical outcomes were considered significant. The principal component (PCA) was done using OriginPro 2023 (Origin Lab, Co., USA).

3. Results and discussion

The physicochemical and structural features of γ-irradiated-PF

The key fiber components

Fig. 1 shows that after γ-irradiation, the cellulose, hemicellulose, and lignin contents of PF were reduced ($p<0.05$) equated with to the non-irradiated one sample in a dose dependent manner. For example, with an increase in γ-irradiation dosage, the amounts of cellulose, hemicellulose, and lignin were reduced ($p<0.05$). For example, 20 kGy declined cellulose, hemicellulose, and lignin by 13.74, 23.41, and 16.6%, orderly. This might be a lignin that combines hemicellulose, H-bonds, and strong covalent connections to create a stable molecule that is wrapped in cellulose, although it is difficult to predict with certainty when this material will decompose outside of controlled situations [12]. Strong energy rays can also encourage the depolymerization of hemicellulose and cellulose, lignin association cracking, and the conversion of a portion of the dietary fiber component into oligosaccharides, which changed the composition of the insoluble dietary fiber in pea and orange [12,17]. Hemicellulose and lignin's monomeric units were damaged by the energy absorbed during the irradiation procedure that causing them to break down into smaller molecules or other free radicals and reduce their concentration [19]. Increased γ-irradiation dosage caused the PF structure to open, exposing cellulose to be damaged and degraded, and reduced the fiber content [30]. The findings demonstrated that γ-irradiation affected the composition of PF by destroying the binding sites and structures of cellulose, hemicellulose, and lignin. Remarkably, it was noted that TDF and IDF significantly declined ($p<0.05$) with further raising doses to 20 kGy. Meanwhile, SDF was declined because of expanding the irradiation dose starting from 5 to 20 kGy. The findings may be that extreme degradation of the polysaccharide chain leads to EtOH-waning to precipitate SDF, causing in declined SDF [31].

Particle size and specific surface area analysis

The average particle size of PF volume reduced with the increase in γ-irradiation dosage equated with the non-irradiated PF (**Fig. 2**). For example, the size of PF was around 130.44 after 20 kGy done which was 145.72 µm in the control one ($p<0.05$). Meanwhile, the specific surface area significantly increased ($p<0.05$) with values of 76.13 and 83.28 m^2/kg in C and 20 kGy PF, orderly. By breaking molecular chains, lowering the average particle size, and increasing the specific surface area, γ-irradiation results in the depolymerization of lignin and hemicellulose in PF (**Fig. 2**).

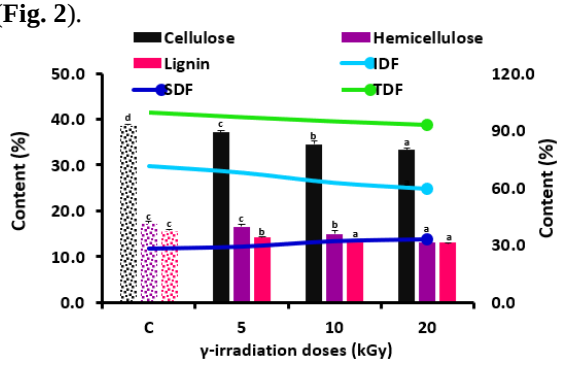

Fig 1. Impact of different doses of γ-irradiation on the key fiber elements of PF.

The irradiation will diminish cellulose and break the glycosidic linkages between it, reducing the size of the dietary fiber particle and increasing the specific surface area of IDF [32]. This suggests that glycosidic linkages may be broken, and fiber components can change during γ-irradiation, affecting the structure and physicochemical characteristics of PF.

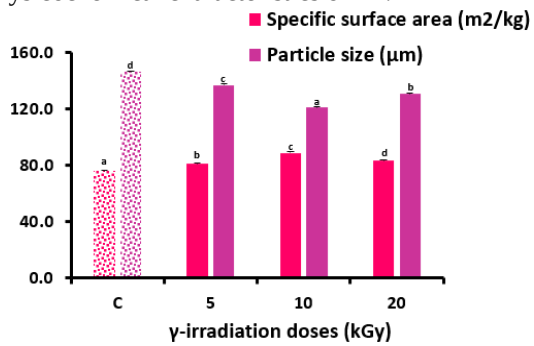

Fig 2. Impact of different doses of γ-irradiation on the specific surface area and particle size of PF.

SEM

Fig. 3 illustrates that the surface microstructure of non-irradiated-PF has a fiber strip structure, while the irradiated-PF had fractures and holes. The pore size of the PF steadily grew as the dosage of γ-irradiation rose from 0 to 20 kGy. The PF's structure had the biggest pores when the radiation dosage was 20 kGy. The PF's pore size decreased as the irradiation dosage grew from 5 kGy to 20 kGy, and when the irradiation dose reached 20 kGy, the PF's surface broke and created a lamellar microstructure, agreeing with our surface area findings (**section 3.1.2**). This may be because an increase in γ-irradiation intensity can break the glycosidic bond in a molecule's chain, lower the molecular weight, and weaken the interaction among molecules. This can encourage the formation of carbonyl and C=O bonds and cause the PF's structure to relax, resulting in a honeycomb structure and larger pores [12]. PFs' reduced particle size and altered microstructure may lead to capillary action and a

greater specific surface area, which may be crucial for the material's ability to absorb various other substances [26]. In addition, it was noted that by disrupting the intermolecular crosslinking of fibers, high-intensity energy field treatment may alter the surface structure and have an impact on the specific surface area [33]. PF develops layered on its surface when the radiation exposure is too great. This could be caused by the build-up of leftover protein on the fiber's surface and fiber fragments that have been damaged because of radiation exposure at a high dosage. The porosity of the fiber structure is mostly responsible for dietary fiber's ability to absorb glucose and retain moisture [34]. This suggests that by modifying microstructure and porosity of PF, proper amount of γ-irradiation may enhance its functional activity.

FTIR

To identify changes in molecular groups and chemical bonds of PF, scientists used FTIR that creates an infrared absorption spectrum based on the vibration of molecules at various wavelengths.

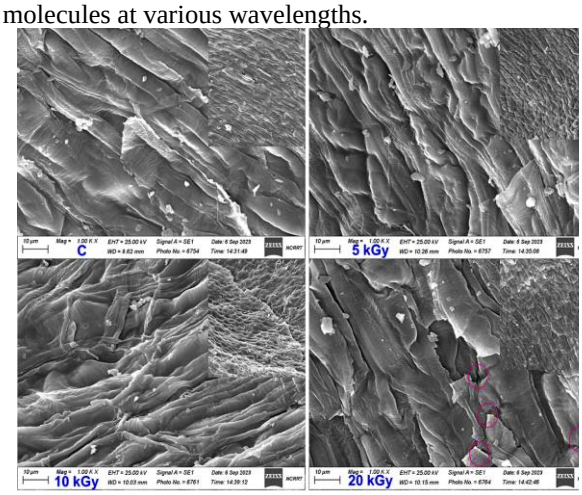

Fig 3. SEM of irradiated and non-irradiated PF with different doses (0, 5, 10, and 20 kGy). The pink circles signify the holes, fissures, and layered structures seen in the irradiated PF.

The kinds of chemical bonds or molecular groups have the greatest influence on the location and intensity of the absorption peak, and induction, conjugation, or steric hindrance modifies the position of the absorption peak [23]. **Fig. 4** shows the spectral curves of all PF, all of which maintained the distinctive bands unique to each technique. The O-H bond tensile vibration causes the absorption bands of all PF in 3500 cm^{-1} range, and these absorption bands also reveal the presence of pectin and hemicellulose in other fibers [12,17]. The asymmetric and symmetrical C-H vibrational bands in the polysaccharide substances methylene were said to be responsible for the absorption peaks around 2930 cm^{-1}, orderly. The existence of a crystalline area was indicated by the absorption peak that was seen at 1240 cm^{-1}. The strength of these absorption bands declined as the dosage of γ-irradiation increased, most likely because of the breakdown of intramolecular H-bonds in cellulose and hemicellulose equated to the non-irradiated PF [35]. The H_2O ability to bind to the fiber matrix became less effective, as seen by the weakening of the absorption peak in 1730 cm^{-1}. Hemicellulose and lignin in PF were damaged by γ-irradiation, as shown by the stretching of C=O and aromatic skeleton of aldehyde/ester groups and the reduction in absorption bands at 1050 cm^{-1}. The physicochemical and functional characteristics of dietary fibers, such as hydration, adsorption, cation exchange capacity, and metal chelation, are significantly influenced by their reactive groups [36], suggesting the possible alteration in physical, chemical, and functional aspects of irradiated-PF.

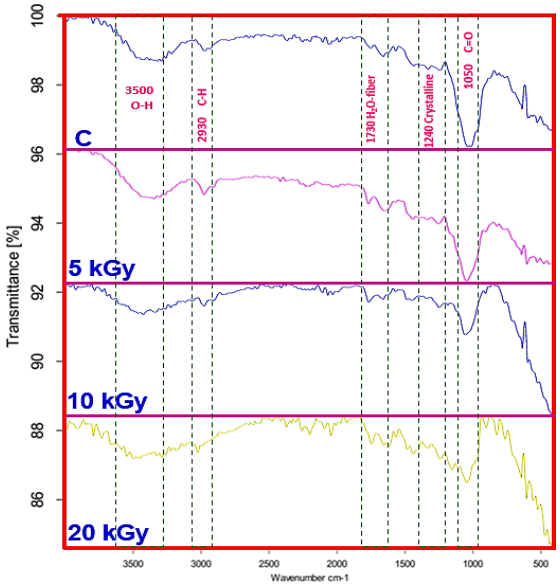

Fig 4. FTIR spectrum of irradiated and non-irradiated PF with different doses (0, 5, 10, and 20 kGy). The green lines signify the key functional groups of PF.

XRD

With the aid of XRD, impact of γ-irradiation on the crystalline features of PF was investigated. The sample's crystal type is indicated by the overall peak form. The increased intensity of the diffraction peak indicates an increase in crystallinity at the diffraction angle. **Fig. 5** shows that the irradiation treatment has negligible effects on peak form and that each PF exhibits distinct absorption peaks at scanning angles (2θ) of 43.22 and 67.58° for the non-irradiated PF. This shows that the cellulose type-I that comprises of ordered crystalline cellulose areas and disordered cellulose and hemicellulose regions, is present in the crystals of all PF. Meanwhile, we have selected both 10 and 20 kGy based PF, where 5 kGy showed no visible effects. 10 and 20 kGy slightly influenced the key XRD peaks of PF, where they kept the original peaks with sight movements, and/or appeared a new peak around 37.58°, confirming the slight effects of γ-irradiation on the cellulose type of PF with slightly

hydrolysing it. This could be because γ-irradiation destroyed both the crystalline and amorphous forms of the material, and the destroyed crystalline form was then broken down into the amorphous form, lowering the crystallinity of PF [16]. As a result, the amorphous region's destruction degree is greater than that of the crystallization region, leading to an increase in crystallinity especially with the high doses of irradiation [12], showing that the crystal structure of irradiated-PF was fluctuated by altering their cellulose, hemicellulose, and lignin contents.

The techno-functional features of irradiated-PF

OHC, WHC, and SC

Dietary fiber's ability to contain oil may make food taste better, last longer on the shelf, and have better sensory qualities [37]. Meanwhile, dietary fiber's great ability to store oil may lessen the absorption of lipids in the intestinal system.

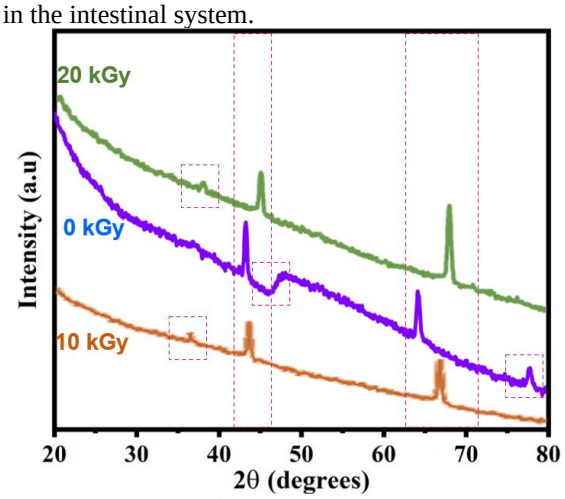

Fig 5. XRD peaks of irradiated and non-irradiated PF with different doses (0, 10, and 20 kGy). The pink squares signify the fluctuations in the main XRD peaks of PF.

Fig. 6 shows that as the dosage of γ-irradiation rose, OHC of PF initially increased and subsequently declined. PF had the maximum OHC when the γ-irradiation dosage was 10 kGy with a value of 8.35 g/g, mostly because the microstructure of PFs may be destroyed during γ-irradiation, increasing porosity and specific surface area [12]. This helps to increase the number of oil droplets that come into touch with and embed in PFs, increasing their ability to retain oil [17]. The pores on the microstructure surface of PF-20 kGy, however, shrank and the specific surface area shrank; thereby, OHC decreased (**Section 3.1.3**).

In food processing, WHC is a functional property that is used to assess the hydration capabilities of dietary fiber [37]. By raising chyme volume and boosting peristalsis, SC and WHC of dietary fiber are advantageous to intestinal function. **Fig. 6** also shows that the SC and WHC of PF were higher than the non-irradiated PF ($p<0.05$). Likewise, SC and WHC rose initially with an increase in γ-irradiation dosage and subsequently dropped with maximum values of 9.35 mL/g and 21.05 g/g in PF-10 kGy, orderly. It demonstrates how dietary fiber's ability to swell and retain H_2O may be improved with the right amount of irradiation (10 kGy). SC of dietary fiber may be influenced by particle size, where the greater SC, the smaller the particle size [17], disagreeing with our particle size findings. Additionally, certain fibers may be broken by mild radiation that would relax the tight network structure of dietary fibers and increase their specific surface area. This is another reason dietary fiber has a higher SC. Dietary fiber's glycosidic bond may be broken by radiation treatment, and at 20 kGy, the PF's microstructure shows noticeable holes and a honeycomb structure. As a result, the PFs' ability to retain water is improved since there is more room for water molecules to be stored. The SC and WHC ability of PF, however, diminished dramatically when the irradiation dosage was 20 kGy. This may be the case since crystallinity and SC are connected. Potato starch that has been irradiation has less crystallinity which lowers its ability to expand [38]. In addition, high-dose irradiation will cause the fibers' network structure to disintegrate, decreasing their ability to store H_2O [17].

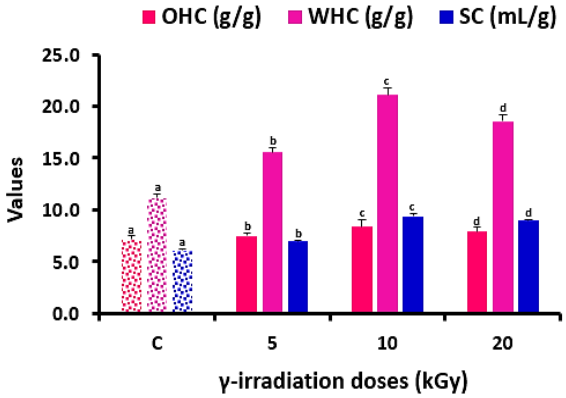

Fig 6. Impact of different doses of γ-irradiation (0, 5, 10, and 20 kGy) on the oil holding capacity (OHC), water holding capacity (WHC), and swelling capacity (SW) of PF.

NAC

Nitrite is a moderately hazardous substance that may combine with other substances to cause cancer [33]. Nitro chemicals that cause cancer in animals may pass through the placenta and have teratogenic effects on the developing baby [39]. The capacity of PF to adsorb nitrite ions is significantly influenced by pH, making it a significant indication. Consequently, NAC of each PF in the simulated stomach and intestinal environments, pH of 2 and 7, orderly. **Fig. 7** demonstrates how pH level and γ-irradiation dosage have an impact on the NAC of PF. NAC at pH of 2 was much greater than that at pH of 7, mostly since in acidic circumstances, NO_2 reacts with H+ to generate HNO_2 that subsequently produces nitrogen oxides, including the molecule N_2O_3 with a significant

electron affinity that may mix with the negatively charged O_2 of phenolic acid groups in PF to cause adsorption [17]. Another explanation is that PF contains active groups that strongly adsorb nitroso groups when exposed to acidic conditions [17]. The nitrite adsorption capacity of PF improves with an increase in radiation dosage before decreasing at two different pH levels with a maximization at 10 kGy to be 212.17 and 106.16 µg/g at pH of 2 and 7, separately. γ-irradiation altered the PFs' structure where their surface looked loose and porous and specific surface area increased, potentially exposing additional nitrite ion adsorption sites. NAC of PF is increased in the gastrointestinal environment following 10 kGy due to the capillary effect created by these pores that speeds up the entrance of nitrite ions into the core of PF's structure.

CAC

The amount of cholesterol in the blood has a direct impact on the development of coronary heart disease. There is evidence that dietary fibre lowers blood cholesterol levels and the risk of cardiovascular disease by preventing the absorption of cholesterol [6,28,36]. Therefore, increasing dietary fiber's ability to absorb cholesterol is crucial.

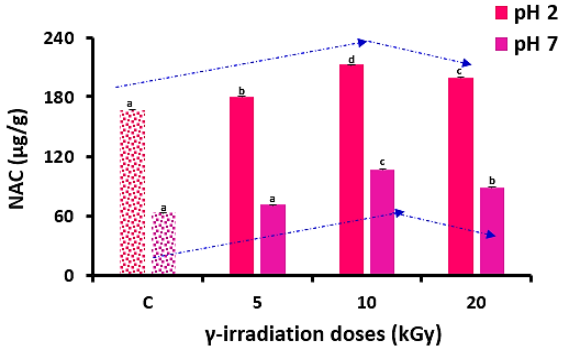

Fig 7. Impact of different doses of γ-irradiation (0, 5, 10, and 20 kGy) on the nitrite adsorption capacity (NAC) of PF at pH values of 2 and 7.

Fig. 8 shows that pH value and γ-irradiation dosage had an impact on the CAC of PF. The CAC of PF rose initially and subsequently reduced at both pH levels in response to an increase in γ-irradiation dosage. The greatest CAC at pHs of 2 and 7 were observed when the γ-irradiation dosage was 10 kGy, with pH of 7 having a larger capacity than that of 2, mainly because of the repulsion between H^+ and certain positive charges in PF and cholesterol under acidic conditions that has an impact on the binding of dietary fiber and cholesterol and reduces the amount of cholesterol adsorption, making CAC of PF in an intestinal environment more efficient than that in a stomach environment. γ-irradiation increases the specific surface area of the IDF from PS when the irradiation dose is around 10 kGy and alters the structure of hemicellulose and lignin to enhance capillary action, increasing the CAC [12,17]. However, wheat 20 kGy, the PF's surface pores, and surface area diminish that decreases the action of capillaries, limiting the CAC of PF and lowering the quantity of cholesterol that is adsorbed.

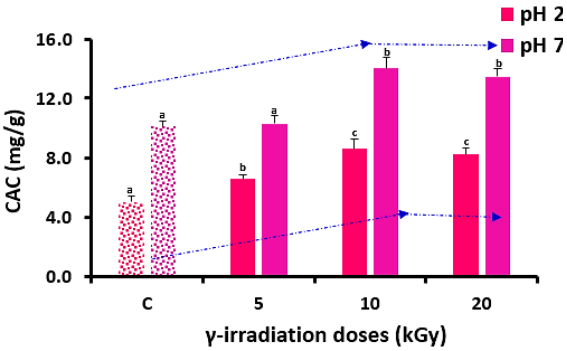

Fig 8. Impact of different doses of γ-irradiation (0, 5, 10, and 20 kGy) on the cholesterol adsorption capacity (CAC) of PF at pH values of 2 and 7.

GAC

A crucial functional property of dietary fiber is that it can delay or inhibit the digestion and absorption of glucose in the gastrointestinal system that helps to lower blood sugar levels [17]. **Fig. 9** demonstrates how glucose concentration (10 and 100 mmol/L) and the dosage of γ-irradiation (0, 5, 10, and 20 kGy) alter the GAC of PF. GAC of PF to various concentrations of glucose initially increased and subsequently declined with the rise in γ-irradiation dosage. GAC of PFs to various concentrations of glucose was highest at 10 kGy, indicating that γ-irradiation could improve the GAC of PF. This may be because moderate irradiation increases specific surface area and porosity, making it easier for glucose to enter the interior of the fiber and bind more tightly to the interior of PF. It was noted that DF enhanced hydration facilitates glucose's bonding to the fiber's surface [12]. Additionally, there was a favourable correlation between GAC and glucose content. This could be because PF's capacity for adsorption is enhanced by the higher contact probability between glucose and fiber. The connection between glucose molecules and the polar and non-polar groups in the PF structure, however, becomes weaker when the irradiation dosage became 20 kGy that lowers the quantity of glucose that may be absorbed [6,12,17].

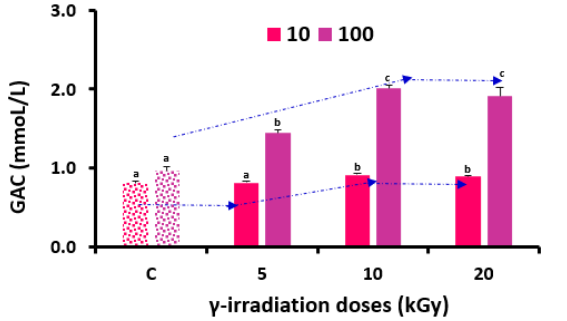

Fig 9. Impact of different doses of γ-irradiation (0, 5, 10, and 20 kGy) on the glucose adsorption capacity (GAC) of PF at a glucose concentration of 10 and 100 mmol/L.

PCA

We performed PCA to find the relationships among parameters. The first and second principal components (PC_1 and PC_2) had individual values of 67.8 and 24.9% with a cumulative variant contribution proportion of 92.7% (>75-85%), separately. PC_1 positively allied with SDF, CAC7-10, SC, GAC2-100, NAC2-7, WHC, OHC, and area (**Fig. 10**). This implied how those parameters are well correlated together, agreeing well with our experimental results. Meanwhile, PC_1 negatively allied with hemicellulose, cellulose, IDF, TDF, lignin, and size. Most notably, PC_1 positively allied with both 10 and 20 kGy treatments, and negatively related with C and 5 kGy, displaying their effects on PF. This also concluded how 10 and 20 kGy treatments are related together. Moreover, location of both 10 and 20 kGy PF together verified their enhancing effects on the features of PF.

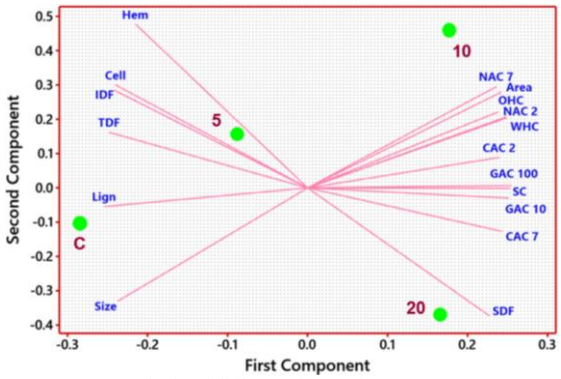

Fig 10. PCA analysis of different doses of γ-irradiation (0, 5, 10, and 20 kGy) and their techno-functional properties.

Conclusions

Using γ-irradiation technology, PF was exposed to various doses (0, 5, 10, and 20 kGy) to study the effects of irradiation dosage on the structural and functional properties of PF. When the -irradiation dose was 20 kGy, the contents of cellulose, hemicellulose, and lignin in PF decreased by 13.74, 23.41, and 16.6%, respectively, and the crystallinity of PF also decreased, according to the structural characteristics of PF. On the surface of the microstructure of the PF subjected to γ-irradiation, pores and amorphous particles were visible. The hemicellulose and lignin in PF were degraded by γ-irradiation, according to infrared spectroscopy studies. According to the functional properties of PF, the maximum OHC, SC, and WHC of PF, 10 kGy had peaked. Likewise, with the GAC, CAC, NAC, 10 kGy had peaked, imply that by altering the structural characteristics of PF using γ-irradiation, the functional qualities of PF may be enhanced. The use of γ-irradiation technology as a pretreatment in this research served as a theoretical foundation for the utilization of PF in food processing.

4. Conflicts of interest

There are no conflicts to declare.

5. Formatting of funding sources

No funding sources.

6. Acknowledgments

The authors would like to thank the Food Technology Department Staffs, Faculty of Agriculture, Benha University for their help.

7. References

[1] 1. Alabaster, O.; Tang, Z.; Frost, A.; Shivapurkar, N. Potential synergism between wheat bran and psyllium: enhanced inhibition of colon cancer. Cancer letters 1993, 75, 53-58.

[2] 2. Fradinho, P.; Nunes, M.C.; Raymundo, A. Developing consumer acceptable biscuits enriched with Psyllium fibre. Journal of food science and technology 2015, 52, 4830-4840.

[3] 3. Verma, A.; Mogra, R. Psyllium (Plantago ovata) husk: a wonder food for good health. International Journal of Science and Research 2013, 4, 1581-1585.

[4] 4. Singh, B. Psyllium as therapeutic and drug delivery agent. International journal of pharmaceutics 2007, 334, 1-14.

[5] 5. Yadav, N.; Sharma, V.; Kapila, S.; Malik, R.K.; Arora, S. Hypocholesterolaemic and prebiotic effect of partially hydrolysed psyllium husk supplemented yoghurt. Journal of Functional Foods 2016, 24, 351-358.

[6] 6. Martellet, M.C.; Majolo, F.; Ducati, R.G.; de Souza, C.F.V.; Goettert, M.I. Probiotic applications associated with Psyllium fiber as prebiotics geared to a healthy intestinal microbiota: A review. Nutrition 2022, 103, 111772.

[7] 7. Jia, W.; Wang, X.; Zhang, R.; Shi, Q.; Shi, L. Irradiation role on meat quality induced dynamic molecular transformation: From nutrition to texture. Food Reviews International 2022, 1-23.

[8] 8. Shahi, S.; Khorvash, R.; Goli, M.; Ranjbaran, S.M.; Najarian, A.; Mohammadi Nafchi, A. Review of proposed different irradiation methods to inactivate food-processing viruses and microorganisms. Food science & nutrition 2021, 9, 5883-5896.

[9] 9. Brum, J.M.; Gibb, R.D.; Peters, J.C.; Mattes, R.D. Satiety effects of psyllium in healthy volunteers. Appetite 2016, 105, 27-36.

[10] 10. Belorio, M.; Gómez, M. Psyllium: A useful functional ingredient in food systems. Critical reviews in food science and nutrition 2021, 62, 527-538.

[11] 11. Franco, E.A.N.; Sanches-Silva, A.; Ribeiro-Santos, R.; de Melo, N.R. Psyllium (Plantago

ovata Forsk): From evidence of health benefits to its food application. Trends in food science & technology 2020, 96, 166-175.
[12] 12. Cheng, T.; Liu, C.; Hu, Z.; Wang, Z.; Guo, Z. Effects of γ-Irradiation on Structure and Functional Properties of Pea Fiber. Foods 2022, 11, 1433.
[13] 13. Kuan, Y.-H.; Bhat, R.; Patras, A.; Karim, A.A. Radiation processing of food proteins–A review on the recent developments. Trends in Food Science & Technology 2013, 30, 105-120.
[14] 14. Joint, F.; Organization, W.H. High-dose irradiation: wholesomeness of food irradiated with doses above 10 kGy: report of a Joint FAO/IAEA/WHO study group; World Health Organization: 1999.
[15] 15. Chmielewski, A.G.; Haji-Saeid, M.; Ahmed, S. Progress in radiation processing of polymers. Nuclear Instruments and Methods in Physics Research Section B: Beam Interactions with Materials and Atoms 2005, 236, 44-54.
[16] 16. Fei, X.; Jia, W.; Wang, J.; Chen, T.; Ling, Y. Study on enzymatic hydrolysis efficiency and physicochemical properties of cellulose and lignocellulose after pretreatment with electron beam irradiation. International journal of biological macromolecules 2020, 145, 733-739.
[17] 17. Li, X.; Wang, B.; Hu, W.; Chen, H.; Sheng, Z.; Yang, B.; Yu, L. Effect of γ-irradiation on structure, physicochemical property and bioactivity of soluble dietary fiber in navel orange peel. Food Chemistry: X 2022, 14, 100274.
[18] 18. Zhu, L.; Yu, B.; Chen, H.; Yu, J.; Yan, H.; Luo, Y.; He, J.; Huang, Z.; Zheng, P.; Mao, X. Comparisons of the micronization, steam explosion, and gamma irradiation treatment on chemical composition, structure, physicochemical properties, and in vitro digestibility of dietary fiber from soybean hulls. Food Chemistry 2022, 366, 130618.
[19] 19. Guo, X.; Zhang, T.; Shu, S.; Zheng, W.; Gao, M. Compositional and structural changes of corn cob pretreated by electron beam irradiation. ACS Sustainable Chemistry & Engineering 2017, 5, 420-425.
[20] 20. Khalifa, I.; Nie, R.; Ge, Z.; Li, K.; Li, C. Understanding the shielding effects of whey protein on mulberry anthocyanins: Insights from multispectral and molecular modelling investigations. International Journal of Biological Macromolecules 2018, 119, 116-124.
[21] 21. Khalifa, I.; Barakat, H.; El-Mansy, H.A.; Soliman, S.A. Enhancing the keeping quality of fresh strawberry using chitosan-incorporated olive processing wastes. Food Bioscience 2016, 13, 69-75, doi:https://doi.org/10.1016/j.fbio.2015.12.008.
[22] 22. Khalifa, I.; Zhu, W.; Nawaz, A.; Li, K.; Li, C. Microencapsulated mulberry anthocyanins promote the in vitro-digestibility of whey proteins in glycated energy-ball models. Food Chemistry 2021, 345, 128805.
[23] 23. Khalifa, I.; Li, M.; Mamet, T.; Li, C. Maltodextrin or gum Arabic with whey proteins as wall-material blends increased the stability and physiochemical characteristics of mulberry microparticles. Food Bioscience 2019, 31, 100445.
[24] 24. Liu, Y.; Zhang, H.; Yi, C.; Quan, K.; Lin, B. Chemical composition, structure, physicochemical and functional properties of rice bran dietary fiber modified by cellulase treatment. Food Chemistry 2021, 342, 128352.
[25] 25. Wang, C.; Li, L.; Sun, X.; Qin, W.; Wu, D.; Hu, B.; Raheem, D.; Yang, W.; Dong, H.; Vasanthan, T. High-speed shearing of soybean flour suspension disintegrates the component cell layers and modifies the hydration properties of okara fibers. Lwt 2019, 116, 108505.
[26] 26. Luo, X.; Wang, Q.; Fang, D.; Zhuang, W.; Chen, C.; Jiang, W.; Zheng, Y. Modification of insoluble dietary fibers from bamboo shoot shell: Structural characterization and functional properties. International Journal of Biological Macromolecules 2018, 120, 1461-1467.
[27] 27. Gan, J.; Huang, Z.; Yu, Q.; Peng, G.; Chen, Y.; Xie, J.; Nie, S.; Xie, M. Microwave assisted extraction with three modifications on structural and functional properties of soluble dietary fibers from grapefruit peel. Food Hydrocolloids 2020, 101, 105549.
[28] 28. Benitez, V.; Rebollo-Hernanz, M.; Hernanz, S.; Chantres, S.; Aguilera, Y.; Martin-Cabrejas, M.A. Coffee parchment as a new dietary fiber ingredient: Functional and physiological characterization. Food Research International 2019, 122, 105-113.
[29] 29. Chen, J.; Zhao, Q.; Wang, L.; Zha, S.; Zhang, L.; Zhao, B. Physicochemical and functional properties of dietary fiber from maca (Lepidium meyenii Walp.) liquor residue. Carbohydrate Polymers 2015, 132, 509-512.
[30] 30. Huang, J.-y.; Liao, J.-s.; Qi, J.-r.; Jiang, W.-x.; Yang, X.-q. Structural and physicochemical properties of pectin-rich dietary fiber prepared from citrus peel. Food Hydrocolloids 2021, 110, 106140.
[31] 31. Loow, Y.-L.; Wu, T.Y.; Yang, G.H.; Md. Jahim, J.; Teoh, W.H.; Mohammad, A.W. Role of energy irradiation in aiding pretreatment of lignocellulosic biomass for improving reducing sugar recovery. Cellulose 2016, 23, 2761-2789.
[32] 32. Al-Sheraji, S.H.; Ismail, A.; Manap, M.Y.; Mustafa, S.; Yusof, R.M.; Hassan, F.A. Purification, characterization and antioxidant

activity of polysaccharides extracted from the fibrous pulp of Mangifera pajang fruits. LWT-Food Science and Technology 2012, 48, 291-296.
[33] 33. Jiang, Y.; Yin, H.; Zheng, Y.; Wang, D.; Liu, Z.; Deng, Y.; Zhao, Y. Structure, physicochemical and bioactive properties of dietary fibers from Akebia trifoliata (Thunb.) Koidz. seeds using ultrasonication/shear emulsifying/microwave-assisted enzymatic extraction. Food Research International 2020, 136, 109348.
[34] 34. Dong, W.; Wang, D.; Hu, R.; Long, Y.; Lv, L. Chemical composition, structural and functional properties of soluble dietary fiber obtained from coffee peel using different extraction methods. Food Research International 2020, 136, 109497.
[35] 35. Wu, C.; Teng, F.; McClements, D.J.; Zhang, S.; Li, Y.; Wang, Z. Effect of cavitation jet processing on the physicochemical properties and structural characteristics of okara dietary fiber. Food Research International 2020, 134, 109251.
[36] 36. Karim, A.; Raji, Z.; Habibi, Y.; Khalloufi, S. A review on the hydration properties of dietary fibers derived from food waste and their interactions with other ingredients: opportunities and challenges for their application in the food industry. Critical Reviews in Food Science and Nutrition 2023, 1-35.
[37] 37. Khalifa, I.; Barakat, H.; El-Mansy, H.A.; Soliman, S.A. Physico-chemical, organolyptical and microbiological characteristics of substituted cupcake by potato processing residues. Food and Nutrition Sciences 2015, 6, 83.
[38] 38. Singh, S.; Singh, N.; Ezekiel, R.; Kaur, A. Effects of gamma-irradiation on the morphological, structural, thermal and rheological properties of potato starches. Carbohydrate polymers 2011, 83, 1521-1528.
[39] 39. Zheng, J.; Stuff, J.; Tang, H.; Hassan, M.M.; Daniel, C.R.; Li, D. Dietary N-nitroso compounds and risk of pancreatic cancer: Results from a large case–control study. Carcinogenesis 2019, 40, 254-262.